Article ID: 1000-324X(2018)05-0582-05 **DOI:** 10.15541/jim20170283

Carbon Quantum Dots/$BiPO_4$ Nanocomposites with Enhanced Visible-light Absorption and Charge Separation

ZHANG Zhi-Jie[1], XU Jia-Yue[1], ZENG Hai-Bo[1,2], ZHANG Na[1]

(1. Institute of Crystal Growth, School of Materials Science and Engineering, Shanghai Institute of Technology, Shanghai 201418, China; 2. Institute of Optoelectronics and Nanomaterials, College of Materials Science and Engineering, Nanjing University of Science and Technology, Nanjing 210094, China)

Abstract: In this study, a CQDs/$BiPO_4$ nanocomposite with enhanced visible-light absorption and charge separation was fabricated *via* a one-step hydrothermal reaction. The photocatalytic activity of the CQDs/$BiPO_4$ nanocomposite was evaluated by degradation of rhodamine B (RhB). The result showed that the CQDs/$BiPO_4$ composite exhibited superior photocatalytic performance to pure $BiPO_4$ under simulated solar light, as well as under visible light irradiation. Its enhanced photocatalytic performance could be ascribed to the excellent light harvesting properties, which increased utilization rate of solar energy, electron transfer efficiency and reservoir ability of the nanocompsites, facilitating the charge separation efficiency of the composite.

Key words: photocatalysis; carbon quantum dots; $BiPO_4$; electron transfer

As a new member of carbon family, carbon quantum dots (CQDs) have attracted much attention due to their unique properties such as strong photoluminescence (PL) emission, broadband optical absorption, chemical stability, good biocompatibility, nontoxity and facile synthesis[1-3]. As a result, they have been extensively used in many fields such as bioimaging, sensors, photodynamic therapy, drug delivery, and energy storage and conversion[4-6]. Recently, CQDs are attracting more and more attention in the field of photocatalysis. Researchers find that besides the traditional down-converted photoluminescence, CQDs also display excellent up-converted photoluminescence (UCPL) properties, which allows for fully exploitation of the solar light[7-8]. Moreover, photoexcited CQDs can also act as electron acceptors and electron donors, since the photoluminescence of CQDs can be quenched efficiently by either electron donor or electron acceptor molecules in solution[9]. Therefore, considering the unique PL behavior and photo-induced electron transfer property, CQDs can perform as an efficient component in the design of high-performance photocatalysts. Up to date, many impressive composite photocatalysts based on CQDs (CQDs/TiO_2, CQDs/ZnO, CQDs/Cu_2O, CQDs/Fe_2O_3, CQDs/Ag_3PO_4, CQDs/C_3N_4) with enhanced photocatalytic activity have been constructed[10-17].

$BiPO_4$ as a new type of oxy-acid salt photocatalyst, is found to exhibit higher photocatalytic activity than TiO_2 under UV light and has attracted increasing interest in the past few years[18-22]. Besides, it also has many advantages such as low cost, nontoxicity, excellent electronic properties and stable chemical structure, which makes it a promising photocatalyst in environmental purification. However, similar to TiO_2, $BiPO_4$ is also a wide band-gap semiconductor (*ca*. 3.85 eV) and suffers from the drawback of narrow photo-response range, which seriously limits its quantum efficiency and practical application. In order to extend the absorption range of $BiPO_4$, various methods have been adopted, including coupling with a narrow band-gap semiconductor[23-26], adjusting the surface oxygen vacancy[27-28] and doping with fluorine[29] or Ag[30-31]. These attempts have successfully extended the photo-absorption range of $BiPO_4$ and enhanced its photocatalytic activity.

In this study, with the purpose of broadening the photo-response and promoting the charge separation of $BiPO_4$ simutaneously, a CQDs/$BiPO_4$ nanocomposite has been designed and fabricated *via* a facile hydrothermal route. Due to the photo-induced electron transfer and electron reservoir properties, as well as the light harvesting abilities of CQDs, the CQDs/$BiPO_4$ composite exhibited enhanced photocatalytic activity in the photodegradation of RhB under both simulated solar light and

Received date: 2017-06-06; **Modified date:** 2017-08-21
Foundation item: National Science Foundation of China (51402194, 51572128); Shanghai Science and Technology Committee (14YF1410700); Shanghai Institute of Technology (BJPY2015-1)
Biography: ZHANG Zhi-Jie (1984–), PhD. E-mail: zjzhang@sit.edu.cn
Corresponding author: XU Jia-Yue, professor. E-mail: xujiayue@sit.edu.cn

visible light (λ > 420 nm). Based on the transient photocurrent response and radicals trapping experiments, a possible mechanism of the improved photocatalytic activity was proposed.

1 Experimental procedures

1.1 Synthesis

CQDs were synthesized according to a procedure reported by Reisner, *et al*[32]. For the synthesis of CQDs/$BiPO_4$ nanocomposite, in a typical process, 4 mmol of $Bi(NO_3)_3{\cdot}5H_2O$ was added into 80 mL distilled water to obtain a white suspension. Then 14.4 mmol of $NaH_2PO_4{\cdot}2H_2O$ was added into the suspension under magnetic stirring. After that, desired amount of CQDs solution (20 mg/mL) was added into the above mixture and stirred continuously for several hours. The resulting suspension was transferred into a Teflon-lined stainless steel autoclave and maintained at 160℃ for 24 h. After it was cooled to room temperature naturally, the products were washed with distilled water for several times and then dried at 60℃ for 12 h. The loading amount of CQDs were 1.6wt%, 2.4wt% and 3.2wt%, respectively.

1.2 Characterization

The crystal structure of the products were characterized by X-ray diffraction (XRD) using an X-ray diffractometer (Rigaku Co. Ltd., Tokyo, Japan). UV–Vis diffuse reflectance spectra of the samples were measured using a PE Lambda 900 UV-Vis spectrophotometer. Morphologies of the as-prepared products were examined by a FEI tecnaiG2F30 electron microscope. The photocurrents were measured on an electrochemical system (CHI 650E, Shanghai Chenhua) using a standard three-electrode cell.

1.3 Photocatalytic test

In order to evaluate the photocatalytic activities of the CQDs/$BiPO_4$ composites, photo-degradation of RhB was performed under simulated solar light using a 500 W Xe lamp as the light source. In a typical procedure, 50 mg of the photocatalyst was dispersed in 50 mL of RhB solution (10^{-5} mol/L), which was magnetically stirred in dark for 60 min to establish the adsorption–desorption equilibrium between RhB and the photocatalyst powders. Upon illumination, 3 mL of suspension was sampled every time intervals and centrifuged to remove the photocatalyst. The concentration change of RhB was analyzed by recording the variations of the absorption band maximum (552 nm) through a UV-Vis PE Lambda 900 spectrophotometer.

2 Results and discussion

2.1 Crystal structure

The XRD patterns of CQDs/$BiPO_4$ nanocomposites with different contents of CQDs are shown in Fig. 1. The XRD profiles of the $BiPO_4$ and CQDs/$BiPO_4$ nanocomposites could be indexed to the pure monoclinic phase (space group P21/n, JCPDS 15-0767). The peaks at 2θ= 27.1°, 29.1°, and 31.2° could be assigned to (200), (120) and (012) crystal planes of monoclinic $BiPO_4$, respectively. No characteristic diffraction peak of carbon is detected for the CQDs/$BiPO_4$ composites, which could be due to the low contents and low crystallinity of CQDs in the CQDs/$BiPO_4$ nanocomposites.

2.2 Morphology

The TEM image of the CQDs/$BiPO_4$ composite (2.4wt%) is exhibited in Fig. 2(a), which reveals that the particles are crystallites with different sizes ranging from 50 nm to several hundred nanometers. The HRTEM image in Fig. 2(b) displays the excellent crystalline structures of $BiPO_4$ nanoparticles and CQDs. The lattice fringe with an interplanar distance of 0.466 nm agrees well with the (011) plane of $BiPO_4$, and the lattice spacing of 0.321 nm and 0.230 nm correspond to the (002) and (100) planes of carbon, respectively.

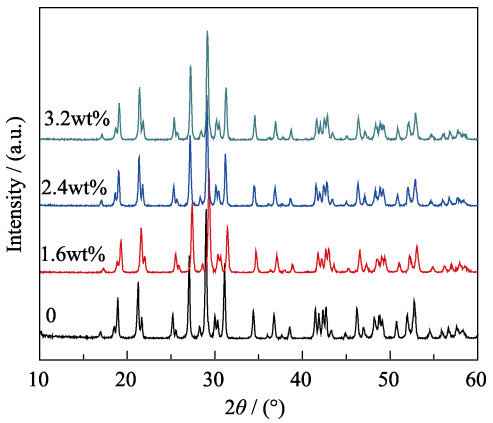

Fig. 1　XRD patterns of pure $BiPO_4$ and CQDs/$BiPO_4$ composites with different amounts of CQDs

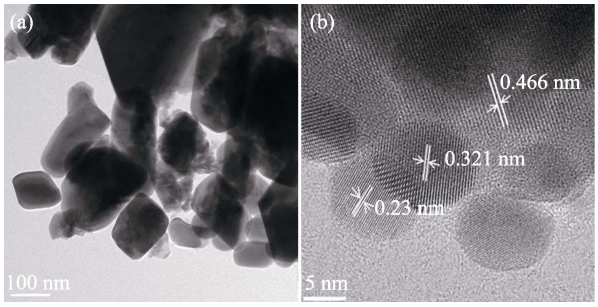

Fig. 2　TEM image of the CQDs/$BiPO_4$ composite (2.4wt%) (a) and high resolution TEM image of the CQDs/$BiPO_4$ composite (b)

2.3 UV-Vis diffuse reflectance spectra

The optical properties of the samples are characterized by UV-Vis diffuse reflectance spectra (DRS) spectra, as shown in Fig. 3. The DRS spectrum of pure $BiPO_4$ clearly displays the band gap absorption onset located at about 320 nm, while the DRS spectra of the CQDs/$BiPO_4$ composites show a slight red shift of the absorption edge. In addition, with increase in the amount of CQDs in the composites, the absorption intensity slightly increases, which can be attributed to the addition of CQDs and can be considered as one of the main factors for the improvement of the photocatalytic performance.

2.4 Photocatalytic activities

To investigate the photocatalytic performance of the as-prepared CQDs/$BiPO_4$ composites, photocatalytic degradation of a model pollutant, RhB is performed under simulated solar light irradiation. Figure 4(a) shows the photocatalytic degradation of RhB *vs*. irradiation time by pure $BiPO_4$ and CQDs/$BiPO_4$ composites with different amounts of CQDs. It can be seen that all the composites display higher photocatalytic activity than pure $BiPO_4$. Moreover, when the mass percentage of CQDs is 2.4wt%, the sample shows the best photocatalytic performance, which can degrade RhB completely after 40 min of irradiation under simulated solar light. In contrast, only 42.8% of RhB is degraded by pure $BiPO_4$ after the same time period. However, further increasing the amount of CQDs leads to an obvious decrease of photocatalytic activity, which can be due to the reason that the higher content of CQDs in the CQDs/$BiPO_4$ composites can result in a competition for light absorption, which decreases the availability of light for RhB degradation.

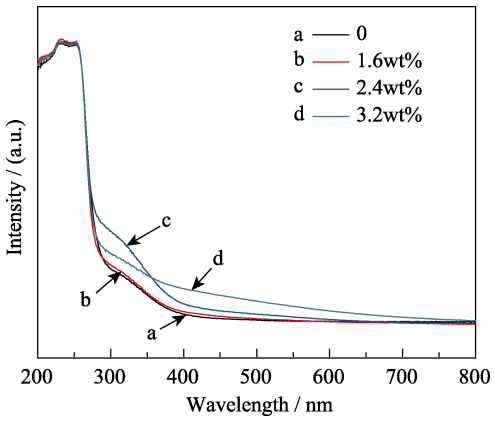

Fig. 3 UV-Vis diffuse reflectance spectra of the as-prepared samples

In addition, photo-degradation of RhB is carried out under visible light (Xe lamp with a band pass filter to remove light with wavelength of λ<420 nm) in order to elucidate the roles of CQDs in the composite. As shown in Fig. 4(b), under visible light irradiation, the CQDs/$BiPO_4$ composite (2.4wt%) exhibits better photocatalytic performance than pure $BiPO_4$, which can degrade 33.3% and 17.7% of RhB after 80 min of visible light irradiation, respectively. Considering the photo-sensitization effect of dyes, a colorless compound phenol is selected as the model pollutant. As shown in Fig. 4(c), under visible light irradiation, the degradation of phenol is negligible by pure $BiPO_4$, while CQDs/$BiPO_4$ composite still exhibits photocatalytic activity in the degradation of phenol. This result demonstrates that CQDs can act as a photo-sensitizer to broaden the photo- absorption range of $BiPO_4$, which leads to the enhanced visible light photocatalytic activity of the CQDs/$BiPO_4$ composite.

2.5 Mechanism of enhanced photo-activities

As well known, the photocatalytic performance is closely related to the generation, separation and migration efficiencies of photogenerated electrons and holes[33], which can be reflected by the photocurrents. Figure 5 shows the photoresponses of pure $BiPO_4$ and CQDs/$BiPO_4$ composite after deposition on FTO electrodes under several on/off sunlight irradiation cycles. It can be seen that both samples exhibit stable and reversible photocurrent at light-on and off. Moreover, the photocurrent generated by CQDs/$BiPO_4$ composite is about 1.9 times as high as that of $BiPO_4$, which implies higher separation efficiency

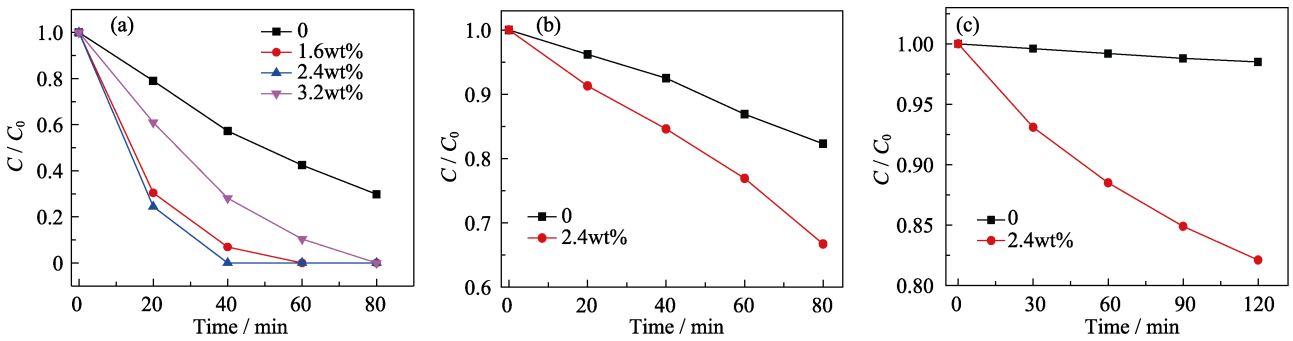

Fig. 4 (a) Degradation efficiency of RhB as a function of time by pure $BiPO_4$ and CQDs/$BiPO_4$ composites with different amounts of CQDs under simulated solar light irradiation; degradation efficiency of RhB (b) and phenol (c) as a function of time by pure $BiPO_4$ and CQDs/$BiPO_4$ composites (2.4wt%) under visible light irradiation (λ>420 nm)

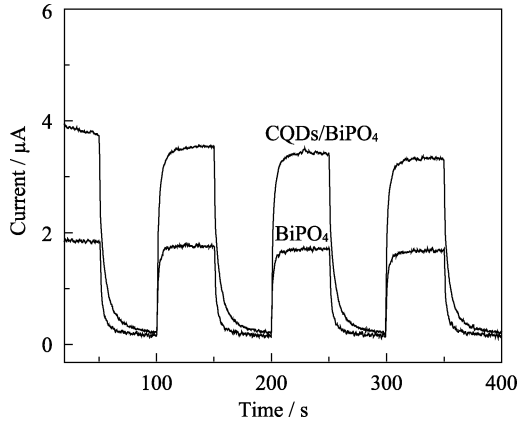

Fig. 5　Transient photocurrent response curves of pure $BiPO_4$ and CQDs/$BiPO_4$ composite (2.4wt%)

and longer lifetime of the photogenerated charge carriers. This is in good agreement with the enhancement of the photocatalytic activity.

In order to further elucidate the photocatalytic mechanism, the main oxidative species in photocatalytic process are detected through the trapping experiments of radicals using EDTA-2Na as holes radical scavenger, tert-butylalcohol (t-BuOH) as hydroxyl radical scavenger, and benzoquinone as superoxide radical ($\cdot O_2^-$) scavenger[34], respectively. As shown in Fig. 6, with the addition of t-BuOH to the reaction system, the photocatalytic activity decreases slightly. In contrast, the addition of EDTA-2Na and benzoquinone cause a severe suppression of the degradation rate. This result demonstrates that holes and superoxide radicals are the main oxidative species in the CQDs/$BiPO_4$ composite system, rather than hydroxyl radicals.

On the basis of the above experimental results, a possible mechanism for the superior photocatalytic performance of CQDs/$BiPO_4$ composite is proposed. Firstly, the introduction of CQDs can extend the photo-response of $BiPO_4$ into the visible range of the solar spectrum,

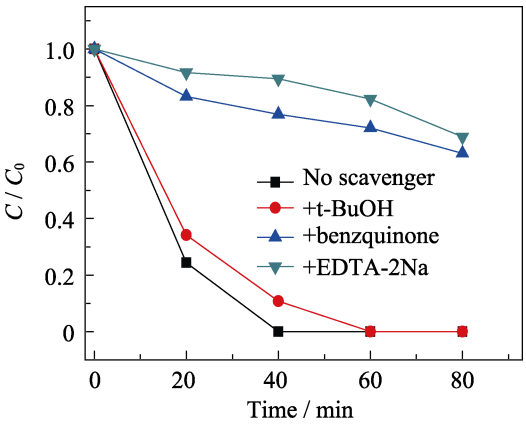

Fig. 6　Photocatalytic degradation of RhB by CQDs/$BiPO_4$ composite (2.4wt%) with different scavengers

thus increasing the utilization rate of solar energy. Secondly, CQDs as an electron reservoir can trap electrons emitted from $BiPO_4$, which can inhibit the recombination rate of the photo-generated charge carriers, as confirmed by the transient photocurrent response shown in Fig. 5. On the other hand, the holes on the valence band of $BiPO_4$ can oxidize the pollutant directly. Overall, CQDs may act as sensitizer and transporter in the CQDs/$BiPO_4$ composite, which not only increase the utilization rate of solar energy, but also promote the separation of the photo-induced charge carriers. Therefore, the CQDs/$BiPO_4$ composite exhibits enhanced photocatalytic activity.

3　Conclusion

In summary, a facile hydrothermal route was dereloped to synthesize CQDs/$BiPO_4$ composite with high photocatalytic activity for pollutant degradation. The results of UV-Visible DRS spectra, photocurrent measurement, as well as the radicals trapping experiments, show that CQDs can act as a photosensitizer and transporter in the CQDs/$BiPO_4$ composite. As a result, the CQDs/$BiPO_4$ composite exhibited enhanced photocatalytic activity in the photodegradation of RhB under simulated solar light, as well as under visible light. Such novel composites may bring new insight into the design of highly efficient visible light photocatalytic systems.

References:

[1] RAY S C, SAHA A, JANA N R, *et al*. Fluorescent carbon nanoparticles: synthesis, characterization, and bioimaging application. *The Journal of Physical Chemistry C*, 2009, **113(43):** 18546–18551.

[2] TANG L B, JI R B, CAO X K, *et al*. Deep ultraviolet photoluminescence of water-soluble self-passivated graphene quantum dots. A*CS Nano*, 2012, **6(6):** 5102–5110.

[3] LI H T, HE X D, LIU Y, *et al*. One-step ultrasonic synthesis of water-soluble carbon nanoparticles with excellent photoluminescent properties. *Carbon*, 2011, **49(2):** 605–609.

[4] YANG S T, CAO L, LUO P G, *et al*. Carbon dots for optical imaging *in vivo*. *Journal of the American Chemical Society*, 2009, **131(32):** 11308–11309.

[5] CAO L, SAHU S, ANILKUMAR P, *et al*. Carbon nanoparticles as visible-light photocatalysts for efficient CO_2 conversion and beyond. *Journal of the American Chemical Society*, 2011, **133(13):** 4754–4757.

[6] SHI W, LI X H, MA H M. A tunable ratiometric pH sensor based on carbon nanodots for the quantitative measurement of the intracellular pH of whole cells. *Angewandte Chemie International Edition*, 2012, **51(26):** 6432–6435.

[7] CAO L, WANG X, MEZIANI M J, *et al*. Carbon dots for multiphoton bioimaging. *Journal of the American Chemical Society*, 2007, **129 (37):** 11318–11319.

[8] SHEN J, ZHU Y, CHEN C, *et al*. Facile preparation and upconversion luminescence of graphene quantum dots. *Chemical Communications*, 2011, **47:** 2580–2582.

[9] LI H T, LIU R H, LIAN S Y, *et al*. Near-infrared light controlled photocatalytic activity of carbon quantum dots for highly selective

oxidation reaction. *Nanoscale*, 2013, **5:** 3289–3297.
[10] MING H, MA Z, LIU Y, *et al*. Large scale electrochemical synthesis of high quality carbon nanodots and their photocatalytic property. *Dalton Transactions*, 2012, **41:** 9526–9531.
[11] YU X J, LIU J J, YU Y C, *et al*. Preparation and visible light photocatalytic activity of carbon quantum dots/TiO_2 nanosheet composites. *Carbon*, 2014, **68:** 718–724.
[12] PAN J Q, SHENG Y Z, ZHANG J X, *et al*. Preparation of carbon quantum dots/TiO_2 nanotubes composites and their visible light catalytic applications. *Journal of Materials Chemistry A*, 2014, **2:** 18082–18086.
[13] YU H, ZHANG H C, HUANG H, *et al*. ZnO/carbon quantum dots nanocomposites: one-step fabrication and superior photocatalytic ability for toxic gas degradation under visible light at room temperature. *New Journal of Chemistry*, 2012, **36:** 1031–1035.
[14] LI H T, LIU R H, LIU Y, *et al*. Carbon quantum dots/Cu_2O composites with protruding nanostructures and their highly efficient (near) infrared photocatalytic behavior. *Journal of Materials Chemistry*, 2012, **22:** 17470–17475.
[15] ZHANG H C, MING H, LIAN S Y, *et al*. Fe_2O_3/carbon quantum dots complex photocatalysts and their enhanced photocatalytic activity under visible light. *Dalton Transactions*, 2011, **40:** 10822–10825.
[16] ZHANG H, HUANG H, MING H, *et al*. Carbon quantum dots/Ag_3PO_4 complex photocatalysts with enhanced photocatalytic activity and stability under visible light. *Journal of Materials Chemistry*, 2012, **22:** 10501–10506.
[17] LIU J, LIU Y, LIU N Y, *et al*. Metal-free efficient photocatalyst for stable visible water splitting *via* a two-electron pathway. *Science*, 2015, **347(6225):** 970–974.
[18] PAN C, ZHU Y. New type of $BiPO_4$ oxy-acid salt photocatalyst with high photocatalytic activity on degradation of dye. *Environmental Science & Technology*, 2010, **44(14):** 5570–5574.
[19] PAN C, ZHU Y. Size-controlled synthesis of $BiPO_4$ nanocrystals for enhanced photocatalytic performance. *Journal of Materials Chemistry*, 2011, **21:** 4235–4241.
[20] PAN C, XU J, WANG Y, *et al*. Dramatic activity of C_3N_4/$BiPO_4$ photocatalyst with core/shell structure formed by self-assembly. *Advanced Functional Materials*, 2012, **22(7):** 1518–1524.
[21] LU B, MA X, PAN C, *et al*. Photocatalytic and photoelectrochemical properties of *in situ* carbon hybridized $BiPO_4$ films. *Applied Catalysis A: General*, 2012, **435–436:** 93–98.
[22] PAN C, XU J, CHEN Y, *et al*. Influence of OH-related defects on the performances of $BiPO_4$ photocatalyst for the degradation of rhodamine B. *Applied Catalysis B: Environmental*, 2012, **115–116:** 314–319.
[23] LV T, PAN L, LIU X, *et al*. Enhanced visible-light photocatalytic degradation of methyl orange by $BiPO_4$–CdS composites synthesized using a microwave-assisted method. *RSC Advances*, 2012, **2:** 12706–12709.
[24] XU H, XU Y, LI H, *et al*. Synthesis, characterization and photocatalytic property of AgBr/$BiPO_4$ heterojunction photocatalyst. *Dalton Transactions*, 2012, **41:** 3387–3394.
[25] LIN H, YE H, XU B, *et al*. Ag_3PO_4 quantum dot sensitized $BiPO_4$: a novel p–n junction Ag_3PO_4/$BiPO_4$ with enhanced visible-light photocatalytic activity. *Catalysis Communications*, 2013, **37:** 55–59.
[26] LIN H, YE H, CHEN S, *et al*. One-pot hydrothermal synthesis of $BiPO_4$/$BiVO_4$ with enhanced visible-light photocatalytic activities for methylene blue degradation. *RSC Advances*, 2014, **4:** 10968–10974.
[27] LV Y, ZHU Y, ZHU Y. Enhanced photocatalytic performance for the $BiPO_{4-x}$ nanorod induced by surface oxygen vacancy. *The Journal of Physical Chemistry C*, 2013, **117(36):** 18520–18528.
[28] LV Y, LIU Y, ZHU Y, *et al*. Surface oxygen vacancy induced photocatalytic performance enhancement of a $BiPO_4$ nanorod. *Journal of Materials Chemistry A*, 2014, **2:** 1174–1182.
[29] LIU Y, LV Y, ZHU Y, *et al*. Fluorine mediated photocatalytic activity of $BiPO_4$. *Applied Catalysis B: Environmental*, 2014, **147:** 851–857.
[30] ZHANG Y, FAN H, LI M, *et al*. Ag/$BiPO_4$ heterostructures: synthesis, characterization and their enhanced photocatalytic properties. *Dalton Transactions*, 2013, **42:** 13172–13178.
[31] FULEKAR M H, SINGH A, DUTTA D P, *et al*. Ag incorporated nano $BiPO_4$: sonochemical synthesis, characterization and improved visible light photocatalytic properties. *RSC Advances*, 2014, **4:** 10097–10107.
[32] MARTINDALE B C M, HUTTON G A M, CAPUTO C A, *et al*. Solar hydrogen production using carbon quantum dots and a molecular nickel catalyst. *Journal of the American Chemical Society*, 2015, **137(18):** 6018–6025.
[33] LIU Y F, YAO W Q, LIU D, *et al*. Enhancement of visible light mineralization ability and photocatalytic activity of $BiPO_4$/BiOI. *Applied Catalysis B: Environmental*, 2015, **163:** 547–553.
[34] YUE D, CHEN D M, WANG Z H, *et al*. Enhancement of visible photocatalytic performances of a Bi_2MoO_6–BiOCl nanocomposite with plate-on-plate heterojunction structure. *Physical Chemistry Chemical Physics*, 2014, **16:** 26314–26321.

增强可见光吸收和电荷分离的碳量子点/$BiPO_4$纳米复合材料

张志洁[1]，徐家跃[1]，曾海波[1,2]，张 娜[1]

(1. 上海应用技术大学 材料科学与工程学院，晶体生长研究所，上海 201418; 2. 南京理工大学 材料科学与工程学院，纳米光电材料研究所，南京 210094)

摘 要: 通过水热法一步合成了具有增强可见光吸收和电荷分离的碳量子点/$BiPO_4$纳米复合光催化材料。通过降解罗丹明 B 染料表征了碳量子点/$BiPO_4$纳米复合材料的光催化性能。结果表明：在模拟太阳光或可见光的照射下，碳量子点/$BiPO_4$复合材料的光催化性能均优于单纯的 $BiPO_4$。碳量子点/$BiPO_4$复合材料光催化性能的提升可归因于碳量子点对可见光的吸收增加了太阳光的利用率，以及碳量子点的电子转移和储存性质提高了材料的电荷分离效率。

关 键 词: 光催化；碳量子点；$BiPO_4$；电子转移

中图分类号: TQ174 **文献标识码:** A